Cellular Bioluminescence Imaging

David K. Welsh and Takako Noguchi

Cold Spring Harb Protoc; doi: 10.1101/pdb.top070607

Topic Introduction

Cellular Bioluminescence Imaging

David K. Welsh and Takako Noguchi

Bioluminescence imaging of live cells has recently been recognized as an important alternative to fluorescence imaging. Fluorescent probes are much brighter than bioluminescent probes (luciferase enzymes) and, therefore, provide much better spatial and temporal resolution and much better contrast for delineating cell structure. However, with bioluminescence imaging there is virtually no background or toxicity. As a result, bioluminescence can be superior to fluorescence for detecting and quantifying molecules and their interactions in living cells, particularly in long-term studies. Structurally diverse luciferases from beetle and marine species have been used for a wide variety of applications, including tracking cells in vivo, detecting protein–protein interactions, measuring levels of calcium and other signaling molecules, detecting protease activity, and reporting circadian clock gene expression. Such applications can be optimized by the use of brighter and variously colored luciferases, brighter microscope optics, and ultrasensitive, low-noise cameras. This article presents a review of how bioluminescence differs from fluorescence, its applications to cellular imaging, and available probes, optics, and detectors. It also gives practical suggestions for optimal bioluminescence imaging of single cells.

Cold Spring Harbor Protocols
www.cshprotocols.org

BIOLUMINESCENCE VERSUS FLUORESCENCE

Bioluminescence is emission of light as a result of an enzymatic reaction in a living organism (see Fig. 1) (Wilson and Hastings 1998; Shimomura 2006; www.lifesci.ucsb.edu/~biolum). As in fluorescence, electrons are excited to a higher energy level, and photons are emitted as the electrons return to their resting level. However, in bioluminescence, the energy to excite the electrons comes from a chemical reaction rather than from exogenous illumination. Bioluminescent enzymes are known as luciferases, and their substrates are known as luciferins.

Longitudinal studies of single cells are powerful because they capture dynamic processes as well as the inherent variability among cells. Live cell imaging using specific fluorescent probes has been especially useful in delineating cell structure and function (Giepmans et al. 2006). Bioluminescent probes (luciferases) have received relatively little attention until recently because they are exceedingly dim by comparison. There is no doubt that the much brighter fluorescent probes are preferable for cellular-imaging applications requiring fine spatial or temporal resolution, or good contrast, all of which require the collection of many photons.

Cellular imaging, however, is increasingly directed toward detecting and quantifying low abundance molecules, their interactions, and their functional activities in live cells over extended periods of time. For such applications, bioluminescence imaging has some important advantages, largely related to the fact that it does not require exogenous illumination. Unlike in fluorescence imaging, there is no photobleaching of emitting molecules, no phototoxicity, and no artificial perturbation of light-sensitive cells (e.g., in the retina). Furthermore, although it is much dimmer, bioluminescence can be up

Adapted from *Imaging: A Laboratory Manual* (ed. Yuste). CSHL Press, Cold Spring Harbor, NY, USA, 2010.

Cite this article as *Cold Spring Harb Protoc*; 2012; doi:10.1101/pdb.top070607

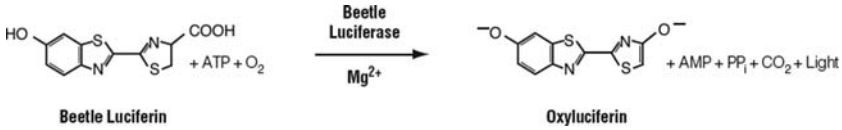

FIGURE 1. Bioluminescent reaction of beetle luciferin. Beetle luciferin substrate is oxidized in a bioluminescent reaction catalyzed by various beetle luciferases such as firefly luciferase (FLuc). The reaction consumes ATP and oxygen, requires the presence of Mg^{++}, and produces light. In the case of FLuc, the light is yellow–green (peak 560 nm) at 20°C and orange (peak ~612 nm) at 37°C (Zhao et al. 2005). (Reprinted, with the kind permission of Promega Corporation, from the Chroma-GloTM Luciferase Assay System Technical Manual #TM062 [http://www.promega.com/tbs/tm062/tm062.html].)

to 50× more sensitive than fluorescence because the background is so low (Arai et al. 2001; Choy et al. 2003; Troy et al. 2004; Dacres et al. 2009).

The exceedingly low background of bioluminescence imaging derives from two factors. First, relative to endogenous fluorescence (autofluorescence), which can sometimes be as bright as the signal itself (Billinton and Knight 2001), endogenous bioluminescence (autoluminescence) of most cells is extremely low (Troy et al. 2004). For example, from a 500-µm hippocampal slice, autoluminescence (related to oxidative metabolism) is only ~3–4 photons/mm^2/sec (Isojima et al. 1995). Second, with bioluminescence, there are no excitation photons, which contribute greatly to background in fluorescence imaging because of scattering and spectral overlap with emission photons. As a result of these two factors, background levels in bioluminescence imaging are exceedingly low, and the signal-to-noise ratio (SNR) can be very high despite the dim signals.

In summary, fluorescence is usually better suited than bioluminescence for precise localization of cellular components or processes over short time periods or for studying processes with rapid dynamics. Bioluminescence, on the other hand, is more sensitive (because of lower background) and less toxic than fluorescence, making it suitable for many live cell applications in which high spatial and temporal resolution is not critical, particularly long-term studies of biological processes with slower dynamics or light-sensitive components.

APPLICATIONS OF BIOLUMINESCENCE

Tracking Molecules and Cells

In recent years, bioluminescent probes have been used for a wide variety of imaging applications (Greer and Szalay 2002; Welsh et al. 2005), including tracking molecules and cells. Firefly luciferase (FLuc) is commonly used for ATP assays, exploiting the ATP requirement for its bioluminescent reaction, and this strategy has been adapted to image ATP release from mammalian cells (Zhang et al. 2008). Protein secretory pathways in cells have been imaged using the secreted *Gaussia* luciferase (Suzuki et al. 2007). Although it has not yet achieved single-cell resolution, a very active application area is tracking cells in whole mice in vivo by imaging (e.g., tumor cells, immune cells, stem cells, bacteria, and viruses) (Dothager et al. 2009). In such applications, the cells are typically engineered to express a luciferase reporter, but the luciferase can also be fused to antibodies directed against desired cell markers (Venisnik et al. 2007).

Protein–Protein Interactions: Bioluminescence Resonance Energy Transfer and Luciferase Complementation Imaging

Protein–protein interactions in single cells can be quantified by two different bioluminescence imaging techniques. In bioluminescence resonance energy transfer (BRET), one protein is tagged with a luminescent photon donor, another protein is tagged with a fluorescent photon acceptor (at a longer wavelength), and close proximity of the two proteins allows the transfer of photons, detected as a change in the emission spectrum (Subramanian et al. 2004). BRET is similar to fluorescence resonance energy transfer (FRET), except that the donor is luminescent rather than fluorescent, so

no exogenous illumination is required. Recent developments in BRET include brighter and redshifted probes (Hoshino et al. 2007; De et al. 2009), improved dynamic range (De et al. 2007), and achievement of subcellular resolution (Coulon et al. 2008). In an alternative approach known as luciferase complementation imaging (LCI), two proteins are tagged with complementary luciferase fragments, and close proximity of the proteins reconstitutes luciferase activity, detected as luminescence (Villalobos et al. 2008). For example, LCI has recently been used to detect epidermal growth factor receptor dimerization (Yang et al. 2009).

Calcium Levels: Aequorin

Calcium can be imaged in cells using variants of aequorin, a calcium-sensitive luciferase found in the jellyfish *Aequorea victoria* (Shimomura et al. 1993). Aequorin acts on its substrate (coelenterazine) in a calcium-dependent manner to produce coelenteramide and the emission of blue (470-nm) light. In the jellyfish, aequorin associates with green fluorescent protein (GFP), and BRET transfer to GFP results in the emission of brighter green light (509 nm), brighter because of higher quantum yield. Mimicking nature, the Brulet group engineered a GFP-aequorin fusion probe that is much brighter and redshifted compared with aequorin alone, can be genetically targeted to particular cell types or organelles, and allows easy preliminary focusing and identification of cells using fluorescence (Baubet et al. 2000). This GFP-aequorin has relatively fast kinetics and a wide dynamic range and is relatively insensitive to pH (Rogers et al. 2005; Curie et al. 2007). Further redshifted variants have been generated recently: Venus-aequorin and red fluorescent protein (RFP)-aequorin (Curie et al. 2007; Manjarrés et al. 2008). Such probes have been used to image calcium in *Drosophila* brain (Martin et al. 2007) and whole mice (Curie et al. 2007; Rogers et al. 2007). Single-cell resolution has been achieved in mammalian neurons and cell lines (Baubet et al. 2000; Rogers et al. 2005, 2008) and in mouse retina (Agulhon et al. 2007). The coelenterazine substrate can be chemically altered to change its sensitivity to calcium, allowing measurement over different concentration ranges (Manjarrés et al. 2008).

Circadian Gene Expression

Luciferases are excellent reporters of gene expression, as illustrated by studies of circadian clock function in cells from an impressive variety of species. This approach was pioneered in the 1950s with studies of the naturally occurring circadian bioluminescence rhythm of *Gonyaulax*, a marine dinoflagellate responsible for some red tides and associated bioluminescent waves (Hastings 1989). In the 1990s, engineered bioluminescent reporters of clock gene expression were used to image circadian clock function in plants (Millar et al. 1992), cyanobacteria (Kondo et al. 1993), and flies (Brandes et al. 1996; Plautz et al. 1997). More recently, single-cell resolution has been achieved in cyanobacteria (Mihalcescu et al. 2004), zebrafish cells (Carr and Whitmore 2005), mouse fibroblasts (Welsh et al. 2004), and neurons from the master circadian pacemaker in the mouse suprachiasmatic nucleus (SCN; see Fig. 2) (Yamaguchi et al. 2003; Liu et al. 2007). In all of these studies, circadian (~24-h) rhythms of bioluminescence could be monitored longitudinally, for days or weeks at a time, and with single-cell resolution in the more recent studies.

Retina

Bioluminescence imaging is particularly well suited for studies of the retina because it does not perturb the retina's light-sensitive physiology with exogenous illumination. A few studies have begun to explore this application (Agulhon et al. 2007; Ruan et al. 2008).

Multiple Colors, Multiple Parameters

Luciferases with different spectral properties have been used to monitor multiple parameters simultaneously in cell populations. Most studies have used spectrophotometry or luminometry (Almond et al. 2003; Nakajima et al. 2004b; Branchini et al. 2005, 2007; Nakajima et al. 2005; Michelini et al. 2008), including one recent study measuring calcium selectively in different organelles with targeted

Cite this article as *Cold Spring Harb Protoc;* 2012; doi:10.1101/pdb.top070607

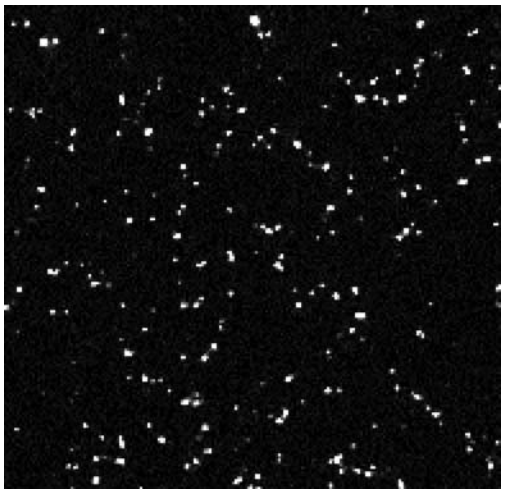

FIGURE 2. Bioluminescent neurons dissociated from the suprachiasmatic nucleus (SCN) of a PER2::LUC knockin mouse (Yoo et al. 2004). Primary SCN neurons were dissociated and cultured for 3 wk under standard conditions (Welsh et al. 1995). The cells were then transferred to HEPES-buffered medium containing 1-mM luciferin and imaged on an inverted Olympus I×70 microscope using a UPlanApo 4× objective and a Spectral Instruments, Inc. SI800 charge-coupled device (CCD) camera cooled to –90°C, with 4 × 4 binning. To eliminate spurious events, this image was constructed by pixelwise minimization of two consecutive 29.9-min exposures. Note the clear luminescence from individual cells, and the visible pixelation (1 pixel = 13 µm), reflecting a deliberate sacrifice of spatial resolution to maximize SNR.

GFP-aequorin and RFP-aequorin (Manjarrés et al. 2008). In the study of circadian clocks, differently colored luciferases have been used to monitor circadian expression of two genes at once in cyanobacteria (Kitayama et al. 2004), to measure effects of RORα on both *Per1* and *Bmal1* gene expression (Nakajima et al. 2004a), and to test for interactions between circadian clocks of two separately labeled populations of Rat-1 fibroblasts (see Fig. 3) (Noguchi et al. 2008). A few studies with differently colored luciferases have used CCD cameras to image cell cultures (Gammon et al. 2006; Davis et al. 2007), plants (Ogura et al. 2005), or *Xenopus* embryos (Hida et al. 2009), but discrimination of multiple luciferase signals has not yet been achieved with single-cell resolution.

Engineered Luciferases: Protease Activity, Ligand Binding, Cyclic AMP

As with fluorescent probes (Giepmans et al. 2006), bioluminescent probes can be engineered to expand their range of uses. For example, protease activity can be assayed by attaching to FLuc an inhibitory peptide, which is cleaved by a specific protease (O'Brien et al. 2005). Other modifications allow FLuc to change its conformation and luminescence activity as a result of protease activity, or on binding rapamycin or cyclic AMP (cAMP)(Fan et al. 2008). These probes have not yet been used for imaging but illustrate the potential for future applications.

LUCIFERASES

Firefly Luciferase

The best known bioluminescent probe is FLuc (Fraga 2008), a 61-kDa monomeric enzyme that catalyzes oxidation of its substrate, beetle luciferin, with the emission of yellow–green light (peak ~560 nm at 25°C; maximum quantum yield 41%; see Fig. 1) (Ando et al. 2008). This reaction requires ATP and oxygen. Optimal pH is 7.8 (Baggett et al. 2004), with reduced light emission at

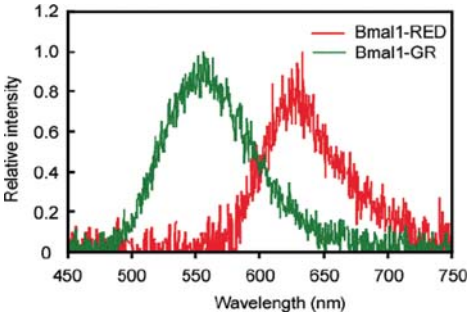

FIGURE 3. Bioluminescence emission spectra of two fibroblast cell lines, one transfected with a green-emitting luciferase from the Japanese luminous beetle (*Rhagophthalmus ohbai*), and the other with a red-emitting luciferase from the railroad worm (*Phrixothrix hirtus*). Luciferases were expressed under control of a promoter from the circadian clock gene *Bmal1* and served as reporters of circadian clock function. Interactions among cellular clocks were tested by simultaneous measurement of circadian oscillations in two separate populations of cells. (Reprinted from Noguchi et al. 2008, with permission, from BioMed Central.)

low pH because of decreased quantum yield (Ando et al. 2008). The reaction rate is also temperature dependent, yielding brighter bioluminescence at 37°C than at 25°C when FLuc is expressed in mammalian cells (Zhao et al. 2005). Interestingly, the emission spectrum is also substantially red-shifted under these conditions (peak ~612 nm [orange] at 37°C) (Zhao et al. 2005). In cells, newly synthesized FLuc is rapidly inactivated by reaction products such as dehydroluciferyl-adenylate (L-AMP) (Fraga et al. 2005), so its functional half-life (as measured by luminescence) is determined partly by this product inhibition (Day et al. 1998) as well as by protein turnover (Leclerc et al. 2000). Estimates of FLuc luminescence half-life in mammalian cells, in the presence of protein synthesis inhibitors, range from ~1 to 4 h (Nguyen et al. 1989; Thompson et al. 1991; Day et al. 1998; Leclerc et al. 2000; Yamaguchi et al. 2003; Baggett et al. 2004). Certain small molecules can also inhibit FLuc, which is a potential source of false positives in high-throughput screens (Auld et al. 2008; Heitman et al. 2008).

Other Luciferases

Many structurally diverse luciferases are found in a wide variety of species, ranging from bacteria to fungi, fish, and insects (Greer and Szalay 2002; Shimomura 2006), but most luciferases used so far in mammalian cells are from beetles (Viviani 2002; Luker and Luker 2008; bioluminescentbeetles.com) or marine species. The bacterial *lux* operon conveniently encodes both luciferase and the enzyme for making its substrate and is used widely for studies in prokaryotes, but has not been successfully expressed in mammalian cells. Among beetles (order Coleoptera), luciferases have been cloned from fireflies (family Lampyridae), click beetles (Elateridae), railroad worms (Phengodidae; named for the paired luminous organs on body segments resembling the lighted windows of a train), and Japanese luminous beetles (Rhagophthalmidae). FLuc is the most extensively studied; other beetle luciferases have different structures but use the same luciferin substrate. Among marine species, luciferases have been cloned from the sea pansy (*Renilla reniformis*), the crystal jellyfish (*A. victoria*), a copepod (*Gaussia princeps*), an ostracod (*Vargula hilgendorfii*), and others. The marine luciferases are smaller, ATP independent, and use a different substrate (coelenterazine), which for several reasons is less desirable for cellular-imaging applications. Compared with beetle luciferin, coelenterazine is more expensive, less soluble, less stable, more toxic, and more autoluminescent, although there are improved synthetic versions (e.g., ViviRen and EnduRen, Promega; www.promega.com/paguide/chap8.htm). *Renilla* luciferase is commonly used with a constitutive promoter as a control in gene expression assays. Jellyfish aequorin can be used to monitor cellular calcium as discussed above. *Gaussia* luciferase is secreted, which makes it suitable only for specialized applications.

Optimizing FLuc

Performance of native FLuc in mammalian cells can be improved in several ways (Paguio et al. 2005). Cytoplasmic expression is obtained by removing a peroxisomal targeting site. Expression levels can be increased by mammalian codon optimization, adding enhancer elements (e.g., SV40) (Yoo et al. 2008) or chimeric introns (Hermening et al. 2004), and introducing multiple copies of the gene (e.g., by transfection, electroporation, viral vectors, or random insertion transgenesis), resulting in brighter bioluminescence. Anomalous expression can be reduced by removing sequences in the FLuc gene and vector backbone that might bind mammalian transcription factors. Sensitivity to rapid dynamics of gene expression, which requires rapid luciferase protein turnover (Wood 1995), can be improved by adding degradation signals (e.g., PEST [proline glutamic acid serine threonine]), although this also sacrifices brightness (Leclerc et al. 2000). Many of these improvements have been incorporated in the *luc2* gene and the PGL4 vectors available from Promega (Paguio et al. 2005).

Faithfulness of bioluminescent reporters of gene expression can be optimized by using the largest possible promoter sequence or (even better) fusing the luciferase gene to the gene of interest and introducing it into its native chromosomal site by homologous recombination, as has been performed for the circadian clock gene *Per2* (Yoo et al. 2004). This knockin strategy includes all transcriptional and posttranscriptional regulatory elements, avoids artifactual effects of the insertion site, and

Cite this article as *Cold Spring Harb Protoc*; 2012; doi:10.1101/pdb.top070607

achieves expression in 100% of targeted cells, but reduces brightness compared with other methods that introduce multiple copies of the gene.

Brighter Luciferases?

Brighter bioluminescent probes would be very useful for cellular imaging, allowing greater spatial and temporal resolutions for a given sensitivity. In the case of fluorescent probes, brighter versions have been engineered by error-prone polymerase chain reaction and directed evolution (Shaner et al. 2004). Theoretically, this same approach could be taken for FLuc, to improve quantum yield, to increase catalytic rate, or to reduce product inhibition. Such efforts have so far been unproductive, however, so FLuc may be nearly optimized already by natural evolution (K. Wood, Promega, pers. comm.). An alternative approach is to search for naturally brighter luciferases from other species (see Table 1). Caribbean click beetle luciferases (CBG [click beetle green], CBR [click beetle red]) appear somewhat brighter than FLuc in mammalian cells, even when carefully normalizing for expression levels (Miloud et al. 2007). Brazilian click beetle luciferase (Emerald luciferase [ELuc]) is claimed to be ~3× brighter than native FLuc, but this may be because of improved expression. *Renilla* and *Gaussia* luciferases (RLuc, GLuc) may also be brighter than FLuc (Stables et al. 1999; Tannous et al. 2005), but they have limitations as discussed above, including higher background autoluminescence. CBG, CBR, and RLuc (like FLuc) are all brighter at 37°C than at 25°C (Zhao et al. 2005). A third approach for obtaining brighter bioluminescent probes is to fuse a luciferase to a fluorescent protein, creating an autoilluminated fluorescent probe in which higher quantum yield is achieved through BRET. Two such probes have been generated: GFP-aequorin (Baubet et al. 2000) and enhanced yellow fluorescent protein (EYFP)-RLuc (Hoshino et al. 2007), both of which have been used for single-cell imaging but that also have limitations associated with their coelenterazine substrate. In principle, FLuc might be similarly fused with an infrared fluorescent protein (Shu et al. 2009); however, FLuc's quantum yield is already fairly high (41%) (Ando et al. 2008), so improvements in brightness are not likely to be dramatic.

Variously Colored Luciferases

For simultaneous monitoring of multiple parameters, luciferases with different spectral properties are available. The emission spectrum of FLuc can be shifted by mutation (Branchini et al. 2005), and

TABLE 1. Luciferases for bioluminescence imaging

Luciferase	Organism	Species name	Emission peak	Supplier	Reference(s)
LuxAB	Bacteria	*Vibrio harveyi*	490 nm	N/A	Kondo et al. (1993)
Luc2, optimized FLuc (firefly)	North American firefly	*Photinus pyralis*	560 nm (~612 nm at 37°C)	Promega (Madison, WI)	Paguio et al. (2005)
CBG	Caribbean click beetle	*Pyrophorus plagiophthalamus*	537 nm	Promega (Madison, WI)	Wood et al. (1989)
CBR	Caribbean click beetle	*P. plagiophthalamus*	613 nm	Promega (Madison, WI)	Wood et al. (1989)
RLuc (*Renilla*)	Sea pansy	*Renilla reniformis*	480 nm	Promega (Madison, WI)	Lorenz et al. (1991)
GLuc (*Gaussia*)	Gaussia	*Gaussia princeps*	480 nm	N/A	Tannous et al. (2005)
GFP-aequorin	Crystal jellyfish	*Aequorea victoria*	509 nm	N/A	Baubet et al. (2000)
EYFP-RLuc	Sea pansy	*R. reniformis*	525 nm	N/A	Hoshino et al. (2007)
ELuc[a] (emerald)	Brazilian click beetle	*Pyrearinus termitilluminans*	538 nm	Toyobo (Osaka, Japan)	Viviani et al. (1999b)
SLG[a]	Japanese luminous beetle	*Rhagophthalmus ohbai*	550 nm	Toyobo (Osaka, Japan)	Nakajima et al. (2005)
SLO[a]	Japanese luminous beetle	*R. ohbai*	580 nm	Toyobo (Osaka, Japan)	Viviani et al. (2001)
SLR[a]	Railroad worm	*Phrixithrix hirtus*	630 nm	Toyobo (Osaka, Japan)	Viviani et al. (1999a), Nakajima et al. (2004b)

N/A, not applicable; CBG, click beetle green; CBR, click beetle red; SLG, stable luciferase green; SLO, stable luciferase orange; SLR, stable luciferase red.

[a]Not commercially available in the United States.

luciferases of various colors are also available from click beetles, railroad worms, Japanese luminous beetles, *Renilla*, and *Gaussia* (see Table 1). Unlike FLuc, the spectral properties of CBG, CBR, and RLuc do not change with temperature (Zhao et al. 2005). Separate signals can be discriminated from differently colored luciferases by using long-pass filters and a spectral unmixing algorithm (see http://www.promega.com/chromacalc). Signals are usually too dim to use the standard narrow-band filters commonly used with fluorescent probes.

OPTICS

Lens Brightness

Bioluminescent probes are much dimmer than fluorescent probes. For optimal bioluminescence imaging of cells, microscope optics must collect and transmit as much light as possible, with minimal magnification so as to concentrate it on a minimal number of camera pixels (Geusz 2001; Christenson 2002; Welsh et al. 2005; Karplus 2006).

The amount of light collected by an objective lens is specified by its numerical aperture (NA),

$$\mathrm{NA} = n \sin \theta, \tag{1}$$

where n is the refractive index of the material between the lens and the sample ($n = 1.00$ for air, 1.33 for water, 1.52 for oil) and θ is the half-angle of the cone of light collected. The fraction of emitted light collected by the lens is its collection efficiency (Q):

$$Q = \mathrm{NA}^2/2n^2. \tag{2}$$

Thus, higher-NA lenses collect more light; they also have better resolving power (distinguish more closely spaced points) but less depth of field. Given the physical constraints of microscope lens design, the practical limit for θ is $\sim 72°$, so maximal NA = 0.95 (air), 1.26 (water), 1.44 (oil); and maximal $Q = 0.45$. Specialized fiber-optic systems can theoretically collect more light ($Q = 0.5$) but require custom fabrication, whereas lenses used for standard 35-mm photography collect much less light ($Q < 0.2$; Karplus 2006).

The proportion of incident light transmitted through a lens is specified by its transmittance, or transmission efficiency. A typical microscope objective lens is composed of approximately eight lens elements, and light is lost to reflection at each optical surface as well as by absorption within each lens element. Reflective losses are minimized by antireflection coatings. Transmittance (T) should be 90% at visible wavelengths.

The brightness (B) of the image is related not only to NA and T but also to magnification (Mag), which determines how widely light is spread across the detector. Higher Mag lenses generally collect more light (because of higher NA) but also spread light over more pixels of the detector, reducing the brightness and the SNR. Thus, lower Mag lenses are brighter for a given NA and also provide greater field of view. Still, modest magnification (4×–10×) is helpful for initial focusing on cells in bright field and for discriminating between adjacent cells:

$$B(\text{luminescence or bright field}) = (\mathrm{NA}/\mathrm{Mag})^2 \times T \times 10^4, \tag{3}$$

$$B(\text{epifluoescence}) = (\mathrm{NA}^2/\mathrm{Mag})^2 \times T \times 10^4. \tag{4}$$

Note that high NA and T are more important for fluorescence than for luminescence. This is because fluorescence brightness depends on how efficiently the objective lens collects and transmits excitation light to the sample as well as how efficiently it collects and transmits emitted light to the detector. Note also that high NA is more important than low Mag for fluorescence, but they are

Cite this article as *Cold Spring Harb Protoc;* 2012; doi:10.1101/pdb.top070607

equally important for luminescence. Hence, whereas the brightest lenses for fluorescence tend to be high Mag, the brightest lenses for luminescence are usually low Mag.

Optics to Maximize SNR

Use the brightest possible objective lens (see Table 2), or use a higher Mag lens with even higher NA and then reduce final Mag with a demagnifying camera adapter. Minimize the number of optical elements in the light path (i.e., no filters or mirrors). Mounting the camera on the bottom port of an inverted microscope instead of on a side port, for example, avoids 2% to 3% attenuation of luminescence by a mirror (R. Nazar, Olympus, pers. comm.). Carefully clean all optical surfaces.

CAMERAS

Detection of Photons

The best detectors for low-light imaging are charge-coupled device (CCD) cameras (Christenson 2002; Karplus 2006), which rely on the photoelectric effect to detect light. When photons impact the silicon chip of a CCD camera, they generate free electrons, which are then channeled in a controlled fashion to a readout amplifier. An analog-to-digital (A/D) converter converts voltage values for perhaps 106 individual picture elements (pixels) to numerical brightness values in arbitrary A/D units, which can be converted to electrons using the gain value supplied by the manufacturer. The sensitivity of the camera is expressed as the quantum efficiency (QE), which is the proportion of incident photons actually detected. Sometimes free electrons are generated in the absence of incident photons (thermal electrons, giving rise to dark current). Dark current (D) is usually reported in units of electrons/pixel/sec.

Camera Noise, Signal-to-Noise Ratio, and Standard Deviation/Mean

Noise in a conventional CCD camera (N_{camera}) originates from two principal sources: the readout process (read noise, N_{read}) and fluctuation of dark current (dark noise, N_{dark}, which increases with exposure duration, t):

$$N_{camera} = \sqrt{(N_{read})^2 + (N_{dark})^2}, \quad (5)$$

$$N_{dark} = \sqrt{Dt}. \quad (6)$$

Useful measures of camera performance for a given sample are the signal-to-noise ratio (SNR; which quantifies the ability to detect faint signals) and the standard deviation (SD)/mean (which quantifies the uncertainty of estimated brightness). The number of incident photons ($P_{incident}$) depends on the sample. The number of detected photons ($P_{detected}$) increases linearly with QE, but the noise associated with the signal (shot noise, N_{shot}) increases only with $\sqrt{P_{detected}}$, so both SNR and

TABLE 2. Microscope objective lenses for bioluminescence imaging

Lens	NA	Mag	T (600 nm)	B
Nikon Plan Apo 4×	0.20	4	0.92	23.0
Nikon Plan Apo 10×	0.45	10	0.88	17.8
Olympus XLFLUOR 4×[a]	0.28	4	0.96	47.0
Olympus UPLSAPO 10×	0.40	10	0.91	14.6
Zeiss FLUAR 5×	0.25	5	0.95	23.8
Zeiss FLUAR 10×	0.50	10	0.93	23.3

[a]Requires nonstandard mounting.

SD/mean improve with brighter samples or higher QE. Of course, SNR also improves with lower camera noise (N_{camera}), so the ideal camera has QE = 100% and $N_{camera} = 0$:

$$P_{detected} = P_{incident} \cdot QE, \tag{7}$$

$$N_{shot} = \sqrt{P_{detected}}, \tag{8}$$

$$N_{total} = \sqrt{(N_{camera})^2 + (N_{shot})^2}, \tag{9}$$

$$SNR = P_{detected}/N_{total}, \tag{10}$$

$$SD/mean = N_{shot}/P_{detected} = \sqrt{P_{detected}}/P_{detected} = 1/\sqrt{P_{detected}}. \tag{11}$$

Conventional CCDs

Conventional CCD cameras designed for low-light imaging have high QE and low dark current but significant read noise. In the back-thinned design, CCD chips are thinned to transparency and illuminated from behind so that photons do not have to penetrate the electron channeling structures on the front of the chip. Also, an antireflection coating is applied to the back of the chip to minimize reflective losses. With this design, QE typically exceeds 90% at wavelengths in which luciferase emission peaks. Cooling the CCD reduces dark current by ~50% for every 7°C–8°C, to values as low as 0.0001 electrons/pixel/sec at temperatures of –90°C or –100°C. Thus, N_{dark} can be <1 electron even for a 60-min exposure. Read noise, however, is typically at least two to three electrons per exposure. Read noise can be minimized by slower readout. Another technique to reduce the impact of read noise is on-chip binning, in which arrays of 2 × 2, 4 × 4, or 8 × 8 pixels are combined and read out as single superpixels. Binning can greatly improve SNR (at the expense of spatial resolution) because superpixels detect more photons than single pixels do but with the same read noise.

Intensified CCDs

Intensified charge-coupled device cameras (ICCDs) use an image intensifier to preamplify the signal above the level of read noise but at the expense of much lower QE in the visible range. ICCDs are composed of a photocathode for detecting incident photons, a microchannel plate (MCP; which is like an array of miniature photomultiplier tubes) for amplification, a phosphor-coated plate to convert amplified electrons back to photons, and a CCD chip to image those amplified photons. QE of the photocathode is only ~40%–50% at best, but amplification by the MCP is so great (>10,000×) that individual photon events greatly exceed the level of CCD read noise, so that a relatively high threshold can be set for counting photons (photon-counting mode), and the read noise is effectively excluded. In the Stanford Photonics XR/Mega-10Z ICCD camera, the GaAsP photocathode has low intrinsic dark current, reduced further by cooling to –20°C, to levels even lower than those of conventional CCD cameras. Amplification noise, arising from fluctuations in intensifier gain, can be reduced by using two MCPs in series such that their fluctuations tend to cancel. Moreover, amplification noise becomes unimportant in photon-counting mode, in which pixel brightness is estimated by the number of photon events above a threshold rather than by the brightness of individual events. ICCDs do have drawbacks: They are expensive and complex, the photocathode and phosphor plate slowly degrade over time, image burn-in can occur, and the camera can be destroyed by accidental exposure to high light levels (although the Stanford Photonics camera has built-in safeguards to prevent this).

Electron-Multiplying CCDs

Like ICCDs, electron-multiplying charge-coupled device cameras (EMCCDs) preamplify the signal above the level of read noise, but they also preserve high QE by using a CCD as the primary detector and an extended gain register within the CCD itself for amplification, instead of a separate image intensifier (Ives 2009). Before readout, free electrons are channeled through approximately 600

Cite this article as *Cold Spring Harb Protoc;* 2012; doi:10.1101/pdb.top070607

high-voltage stages to generate additional electrons by impact ionization. This preamplification effectively excludes read noise in photon-counting mode, as in ICCDs, but impact ionization introduces additional noise arising from clock-induced charge (CIC), which is amplified along with the signal. This CIC noise (N_{CIC}), which occurs with every readout, is typically much lower than a conventional CCD camera's read noise, but it increases with binning and can add up quickly with the frequent exposures needed to avoid overlapping events in photon counting. As in ICCDs, there also is amplification noise, which can be overcome by photon counting. However, because amplification levels in EMCCDs are relatively modest (e.g., 500×–1000×), photon counting may not be as clean in EMCCDs as it is in ICCDs. Dark current also tends to be higher than in other types of CCDs:

$$N_{CIC} = \sqrt{CIC}. \quad (12)$$

Comparisons

Conventional CCDs, ICCDs, and EMCCDs have different strengths and limitations for low-light imaging (see Table 3). Conventional CCDs are simple to operate and perform well when long exposures are feasible, but the high read noise penalty with each exposure limits their use for studying rapidly changing cellular processes. In contrast, ICCDs and EMCCDs are well suited for studying dynamic processes because they preamplify the signal above the read noise, which eliminates or reduces the penalty for frequent exposures. In fact, in the photon-counting mode, exposures must be kept fairly short to avoid overlapping events. This is potentially cumbersome if one needs to do long integrations, constructed from many separate exposures, but allows great flexibility in choosing the integration interval, even after the experiment ends. ICCDs are more complex, more expensive, more difficult to use, and less sensitive than conventional CCDs (QE $\leq$ 50% vs. > 90%), but they make up for their reduced sensitivity by eliminating read noise, thereby preserving high SNR. The Stanford Photonics ICCD camera also has very low dark current, making its SNR performance competitive with conventional CCDs even at long exposure durations. The low QE might still be a disadvantage, however, because collecting fewer photons increases the variability of brightness estimates (SD/mean). Like ICCDs, EMCCDs can effectively eliminate read noise by preamplification, and yet they still have high QE comparable to conventional CCDs. However, EMCCDs introduce a significant new type of noise caused by CIC, cannot count photons as cleanly as ICCDs, and have relatively high dark current.

Testing

Before purchasing a low-light camera, one should test it in a specific application, because performance cannot always be predicted from published specifications. Artifacts caused by subtle defects in the design of camera control hardware or software may be apparent only at very low light levels. For example, some cameras suffer from nonuniform bias (pixel intensities show a distinct pattern on short exposures with shutter closed), latent image (cooled electrons fail to move off the chip during readout), or an excessive number of hot pixels (artifactually bright values).

TABLE 3. Cameras for bioluminescence imaging

Manufacturer	Model	Type	QE(600 nm)	N_{read} or N_{CIC} (electron, rms)	D (electrons/pixel/sec)	Website
Andor Technology	iKon-M 934 (DU934N-BV)	CCD	0.92	2.5	0.000120	andor.com
Spectral Instruments, Inc.	Series 800/850	CCD	0.92	2.9	0.000200	specinst.com
Stanford Photonics	XR/Mega-10Z	ICCD	0.40	0	0.000038	stanfordphotonics.com
Andor Technology	iXon+ 888	EMCCD	0.92	0.071	0.001000	andor.com, emccd.com
Hamamatsu Photonics	ImagEM-1K (C9100-14)	EMCCD	0.92	0.071	0.001000	hamamatsu.com
Photometrics	Evolve	EMCCD	0.92	0.067	0.001000	evolve-emccd.com

rms, root mean square.

Measure read noise (Nr_{ead}; N_{CIC} for an EMCCD camera) by taking a 0-sec exposure with the shutter closed and computing the SD of pixel intensity values across the image. Convert from analog-to-digital units (ADUs) to electrons using the gain of the camera supplied by the manufacturer. Measure total camera noise (N_{camera}) by taking a 30–60-min exposure with the shutter closed and computing the noise in a similar fashion. Dark noise (N_{dark}) and dark current (D) can then be calculated from Equations 5 and 6.

For ICCD or EMCCD cameras in photon-counting mode, count dark events (shutter closed) for various exposure durations (e.g., 0, 1, and 10 sec). For EMCCD cameras, noise in very short exposures is primarily caused by CIC. In photon-counting mode, exposure duration must be kept short to avoid overlapping events, so simulate long exposures by adding events from a series of short exposures. Calculate noise for each exposure duration as the square root of the number of dark events per pixel.

Camera Settings to Maximize SNR

Even with an ideal detector, one must collect enough photons to overcome shot noise. To maximize the signal from dim samples, use the greatest possible on-chip binning and the longest possible exposure (i.e., sacrifice spatial and temporal resolution). To minimize camera read noise, use on-chip binning and the slowest readout speed. To minimize dark current, cool the CCD to the lowest possible temperature. With ICCDs and EMCCDs, turn amplification up high enough so that single photon events are well above read noise, and use the photon-counting mode.

Integrated Systems

Recently, integrated bioluminescence-imaging systems have become available in Japan and Europe. These consist of a small microscope in a light-tight box, an environmental chamber for temperature control and gassing of cultures on the microscope stage, optimized optics, and an EMCCD camera. The optics consist of a high-NA lens system and a straight optical path to the camera. The Olympus Luminoview LV200 and the ATTO Cellgraph systems are both well suited for cellular bioluminescence imaging.

CELL CULTURE AND ENVIRONMENT

Cell Culture

Optimal bioluminescence requires well-oxygenated, healthy cells. For imaging with FLuc reporters, we typically culture tissue explants or dissociated cells in a 35-mm dish containing HEPES-buffered, air-equilibrated Dulbecco's modified Eagle's medium (DMEM; GIBCO 12100-046), supplemented with 1.2 g/L $NaHCO_3$, 10 mM HEPES buffer, 4 mM glutamine, 25 U/mL penicillin, 25 µg/mL streptomycin, 2% B-27 (GIBCO 17504-044), and 1 mM luciferin (BioSynth L-8220). Neurons are cultured in wells of glass-bottomed dishes (MatTek). Brain slices are cultured on Millicell-CM membrane inserts (Millipore/Fisher Scientific PICMORG50). The dish is covered by a 40-mm circular coverslip (Erie Scientific 40CIR1) sealed with vacuum grease to prevent evaporation. It is placed inside a heated lucite chamber (Solent Scientific, UK) custom engineered to fit around the stage of our inverted microscope (Olympus IX71), which rests on an antivibration table (Technical Manufacturing Corporation). The environmental chamber keeps the stage at a constant 36°C. The chamber also accommodates gassing with 5% CO_2 for pH control of bicarbonate-buffered media, if necessary.

Luciferin

Luciferin remains active for up to 6 wk in culture medium at 36°C, without replenishment (D.K. Welsh and S.A. Kay, unpubl.). We recommend D-luciferin from BioSynth or Promega, stored in 100-mM aliquots at –20°C in the dark, used at 0.1–1 mmM. Poorer quality products may contain

Cite this article as *Cold Spring Harb Protoc*; 2012; doi:10.1101/pdb.top070607

L-luciferin, which inhibits the bioluminescence reaction (Nakamura et al. 2005). For neurons, the sodium salt of luciferin may be less toxic than the potassium salt, which is depolarizing. The optimal concentration of luciferin is ~1 mM, which is near saturating for FLuc (1–5 mM) but below the toxic range for most cells (≥2 mM; E. Hawkins, Promega, pers. comm.).

Phenol Red

The pH indicator phenol red can attenuate luminescence by absorbing photons, but, in practice, the effect is minimal for imaging applications. Phenol red has an absorbance peak at ~560 nm, near the emission peaks of FLuc (560 nm) and CBG (537 nm), and very little absorbance in the red at any pH (Duggleby and Northrop 1989). Accordingly, in cell lysates assayed at 20°C in a luminometer, phenol red (15 mg/L) attenuates FLuc (yellow–green) and CBG (green) luminescence by 40%–45% but does not attenuate CBR (red) luminescence appreciably (Promega Bright-Glo and Chroma-Glo manuals). In fibroblasts at pH 7.4 and 37°C, however, FLuc luminescence is redshifted (Zhao et al. 2005), and in luminometer experiments under these conditions, we find that phenol red (15 mg/L) attenuates FLuc luminescence more modestly (25%; T. Noguchi and D.K. Welsh, unpubl.). Furthermore, in imaging experiments using an inverted microscope, much less medium is interposed between cells and detector than is the case in a luminometer. In this configuration, attenuation of FLuc luminescence by phenol red is negligible (T. Noguchi and D.K. Welsh, unpubl.). We often include phenol red (15 mg/L) in culture media for both luminometer and imaging experiments.

Dark Room

Stray light can add significantly to noise levels in bioluminescence imaging. Therefore, it is important to place the imaging setup in a completely dark room with black walls, no windows, and a tightly fitting door with a floor-to-ceiling curtain inside. Avoid any phosphorescent materials (e.g., some paints and plastics). After focusing, cover the culture dish with a small black lucite box, drape the microscope with black cloth (Thorlabs BK5), and turn off room lights and computer monitor. Cover instrument light-emitting diodes (LEDs) with black electrical tape. Test for light leaks by eye after 20-min dark adaptation.

IMAGE PROCESSING

Artifacts

Low-light images should be corrected for various camera artifacts. Artifacts unrelated to the signal that do not change over time (hot pixels, patterned bias, patterned dark current) can be removed by subtracting a dark image (shutter closed, same exposure duration). A nonuniform pattern of QE or amplification can be removed using a flat field image (uniform illumination): Multiply all pixels by the average intensity of the flat field image, and then divide (pixelwise) by the flat field image. Bright spot artifacts are caused by cosmic rays (Butt 2009) or camera-related spurious events. These bright spots are randomly placed and can, therefore, be removed by pixelwise minimization of successive images; that is, by constructing a new image from each pair of images in the time series, taking each pixel of the new image from the dimmer of the two corresponding pixels in the original images. Alternatively, filter out cosmic rays by excluding events above a certain brightness threshold. The latter method works best with ICCD/EMCCD photon counting.

Cell Brightness

Bioluminescence images can be analyzed to produce a time series of luminescence intensity values for multiple individual cells. This requires defining a region of interest for each cell, in each image. The region can be moved, if necessary, to track cells over time but should not change size. For each cell and each image, measure the average intensity in the cell region (Cell), subtract the average intensity of a

background region with no cells (Background), and multiply by the area of the cell region (Area, in pixels), to give cell brightness in A/D units (ADUs). Cell brightness can then be converted to incident photons/min using the camera's gain (Gain, in ADUs/electron) and QE (electrons/photon), and the exposure duration (Exp, in minutes):

$$\mathrm{ADU} = (\mathrm{Cell} - \mathrm{Background}) \cdot \mathrm{Area}, \tag{13}$$

$$\mathrm{photon/min} = \mathrm{ADU}(\mathrm{gain} \cdot \mathrm{QE} \cdot \mathrm{Exp}). \tag{14}$$

CONCLUSION

In summary, bioluminescence imaging is a highly sensitive, nontoxic analytical technique that has proven its utility in a wide range of live cell studies. For optimal results, it requires careful selection and use of luciferase probes, microscope optics, and low-light cameras. In the future, brighter, variously colored luciferases engineered for specific applications, and more sensitive detectors, will further expand the range of applications for bioluminescence imaging.

ACKNOWLEDGMENTS

Thanks to Woody Hastings and Hugo Fraga (Harvard), Keith Wood (Promega), Gary Sims (Spectral Instruments), Mike Buchin (Stanford Photonics), Butch Moomaw (Hamamatsu), Chris Campillo (Andor Technology), and Deepak Sharma (Photometrics) for helpful discussions. Supported by National Institutes of Health grant R01 MH082945 (D.K.W.) and a V.A. Career Development Award to D.K.W.

REFERENCES

Agulhon C, Platel JC, Kolomiets B, Forster V, Picaud S, Brocard J, Faure P, Brulet P. 2007. Bioluminescent imaging of Ca^{2+} activity reveals spatiotemporal dynamics in glial networks of dark-adapted mouse retina. *J Physiol* **583:** 945–958.

Almond B, Hawkins E, Stecha P, Garvin D, Paguio A, Butler B, Beck M, Wood M, Wood K. 2003. A new luminescence: Not your average click beetle. *Promega Notes* **85:** 11–14.

Ando Y, Niwa K, Yamada N, Enomoto T, Irie T, Kubota H, Ohmiya Y, Akiyama H. 2008. Firefly bioluminescence quantum yield and colour change by pH-sensitive green emission. *Nat Photonics* **2:** 44–47.

Arai R, Nakagawa H, Tsumoto K, Mahoney W, Kumagai I, Ueda H, Nagamune T. 2001. Demonstration of a homogeneous noncompetitive immunoassay based on bioluminescence resonance energy transfer. *Anal Biochem* **289:** 77–81.

Auld DS, Thorne N, Nguyen DT, Inglese J. 2008. A specific mechanism for nonspecific activation in reporter-gene assays. *ACS Chem Biol* **3:** 463–470.

Baggett B, Roy R, Momen S, Morgan S, Tisi L, Morse D, Gillies RJ. 2004. Thermostability of firefly luciferases affects efficiency of detection by in vivo bioluminescence. *Mol Imaging* **3:** 324–332.

Baubet V, Le Mouellic H, Campbell AK, Lucas-Meunier E, Fossier P, Brulet P. 2000. Chimeric green fluorescent protein-aequorin as bioluminescent Ca^{2+} reporters at the single-cell level. *Proc Natl Acad Sci* **97:** 7260–7265.

Billinton N, Knight AW. 2001. Seeing the wood through the trees: A review of techniques for distinguishing green fluorescent protein from endogenous autofluorescence. *Anal Biochem* **291:** 175–197.

Branchini BR, Southworth TL, Khattak NF, Michelini E, Roda A. 2005. Red- and green-emitting firefly luciferase mutants for bioluminescent reporter applications. *Anal Biochem* **345:** 140–148.

Branchini BR, Ablamsky DM, Murtiashaw MH, Uzasci L, Fraga H, Southworth TL. 2007. Thermostable red and green light-producing firefly luciferase mutants for bioluminescent reporter applications. *Anal Biochem* **361:** 253–262.

Brandes C, Plautz JD, Stanewsky R, Jamison CF, Straume M, Wood KV, Kay SA, Hall JC. 1996. Novel features of *Drosophila period* transcription revealed by real-time luciferase reporting. *Neuron* **16:** 687–692.

Butt Y. 2009. Beyond the myth of the supernova-remnant origin of cosmic rays. *Nature* **460:** 701–704.

Carr AJ, Whitmore D. 2005. Imaging of single light-responsive clock cells reveals fluctuating free-running periods. *Nat Cell Biol* **7:** 319–321.

Choy G, O'Connor S, Diehn FE, Costouros N, Alexander HR, Choyke P, Libutti SK. 2003. Comparison of noninvasive fluorescent and bioluminescent small animal optical imaging. *BioTechniques* **35:** 1022–1026, 1028–1030.

Christenson MA. 2002. Detection systems optimized for low-light chemiluminescence imaging. In *Luminescence biotechnology: Instruments and applications* (ed Van Dyke K, et al.), pp. 469–480. CRC, Boca Raton, FL.

Coulon V, Audet M, Homburger V, Bockaert J, Fagni L, Bouvier M, Perroy J. 2008. Subcellular imaging of dynamic protein interactions by bioluminescence resonance energy transfer. *Biophys J* **94:** 1001–1009.

Curie T, Rogers KL, Colasante C, Brulet P. 2007. Red-shifted aequorin-based bioluminescent reporters for in vivo imaging of Ca^{2+} signaling. *Mol Imaging* **6:** 30–42.

Dacres H, Dumancic MM, Horne I, Trowell SC. 2009. Direct comparison of bioluminescence-based resonance energy transfer methods for monitoring of proteolytic cleavage. *Anal Biochem* **385:** 194–202.

Davis RE, Zhang YQ, Southall N, Staudt LM, Austin CP, Inglese J, Auld DS. 2007. A cell-based assay for IκBα stabilization using a two-color dual luciferase-based sensor. *Assay Drug Dev Technol* **5:** 85–103.

Day RN, Kawecki M, Berry D. 1998. Dual-function reporter protein for analysis of gene expression in living cells. *BioTechniques* **25:** 848–856.
De A, Loening AM, Gambhir SS. 2007. An improved bioluminescence resonance energy transfer strategy for imaging intracellular events in single cells and living subjects. *Cancer Res* **67:** 7175–7183.
De A, Ray P, Loening AM, Gambhir SS. 2009. BRET3: A red-shifted bioluminescence resonance energy transfer (BRET)-based integrated platform for imaging protein-protein interactions from single live cells and living animals. *FASEB J* **23:** 2702–2709.
Dothager RS, Flentie K, Moss B, Pan MH, Kesarwala A, Piwnica-Worms D. 2009. Advances in bioluminescence imaging of live animal models. *Curr Opin Biotechnol* **20:** 45–53.
Duggleby RG, Northrop DB. 1989. Quantitative analysis of absorption spectra and application to the characterization of ligand binding curves. *Experientia* **45:** 87–92.
Fan F, Binkowski BF, Butler BL, Stecha PF, Lewis MK, Wood KV. 2008. Novel genetically encoded biosensors using firefly luciferase. *ACS Chem Biol* **3:** 346–351.
Fraga H. 2008. Firefly luminescence: A historical perspective and recent developments. *Photochem Photobiol Sci* **7:** 146–158.
Fraga H, Fernandes D, Fontes R, Esteves da Silva JC. 2005. Coenzyme A affects firefly luciferase luminescence because it acts as a substrate and not as an allosteric effector. *FEBS J* **272:** 5206–5216.
Gammon ST, Leevy WM, Gross S, Gokel GW, Piwnica-Worms D. 2006. Spectral unmixing of multicolored bioluminescence emitted from heterogeneous biological sources. *Anal Chem* **78:** 1520–1527.
Geusz ME. 2001. Bioluminescence imaging of gene expression in living cells and tissues. In *Methods in cellular imaging* (ed Periasamy A), pp. 395–408. Oxford University Press, Oxford.
Giepmans BN, Adams SR, Ellisman MH, Tsien RY. 2006. The fluorescent toolbox for assessing protein location and function. *Science* **312:** 217–224.
Greer LF 3rd, Szalay AA. 2002. Imaging of light emission from the expression of luciferases in living cells and organisms: A review. *Luminescence* **17:** 43–74.
Hastings JW. 1989. Chemistry, clones, and circadian control of the dinoflagellate bioluminescent system. The Marlene DeLuca memorial lecture. *J Biolumin Chemilumin* **4:** 12–19.
Heitman LH, van Veldhoven JP, Zweemer AM, Ye K, Brussee J, IJzerman AP. 2008. False positives in a reporter gene assay: Identification and synthesis of substituted *N*-pyridin-2-ylbenzamides as competitive inhibitors of firefly luciferase. *J Med Chem* **51:** 4724–4729.
Hermening S, Kugler S, Bahr M, Isenmann S. 2004. Increased protein expression from adenoviral shuttle plasmids and vectors by insertion of a small chimeric intron sequence. *J Virol Methods* **122:** 73–77.
Hida N, Awais M, Takeuchi M, Ueno N, Tashiro M, Takagi C, Singh T, Hayashi M, Ohmiya Y, Ozawa T. 2009. High-sensitivity real-time imaging of dual protein–protein interactions in living subjects using multicolor luciferases. *PLoS ONE* **4:** e5868. doi: 10.1371/journal.pone.0005868.
Hoshino H, Nakajima Y, Ohmiya Y. 2007. Luciferase-YFP fusion tag with enhanced emission for single-cell luminescence imaging. *Nat Methods* **4:** 637–639.
Isojima Y, Isoshima T, Nagai K, Kikuchi K, Nakagawa H. 1995. Ultraweak biochemiluminescence detected from rat hippocampal slices. *NeuroReport* **6:** 658–660.
Ives D. 2009. Electron multiplication CCDs for astronomical applications. *Nucl Instrum Methods Phys Res A* **604:** 38–40.
Karplus E. 2006. Advances in instrumentation for detecting low-level bioluminescence and fluorescence. In *Photoproteins in bioanalysis* (ed Daunert S, Deo SK), pp. 199–223. Wiley-VCH, Weinheim, Germany.
Kitayama Y, Kondo T, Nakahira Y, Nishimura H, Ohmiya Y, Oyama T. 2004. An in vivo dual-reporter system of cyanobacteria using two railroad-worm luciferases with different color emissions. *Plant Cell Physiol* **45:** 109–113.
Kondo T, Strayer CA, Kulkarni RD, Taylor W, Ishiura M, Golden SS, Johnson CH. 1993. Circadian rhythms in prokaryotes: Luciferase as a reporter of circadian gene expression in cyanobacteria. *Proc Natl Acad Sci* **90:** 5672–5676.
Leclerc GM, Boockfor FR, Faught WJ, Frawley L. 2000. Development of a destabilized firefly luciferase enzyme for measurement of gene expression. *BioTechniques* **29:** 590–598.
Liu AC, Welsh DK, Ko CH, Tran HG, Zhang EE, Priest AA, Buhr ED, Singer O, Meeker K, Verma IM, et al. 2007. Intercellular coupling confers robustness against mutations in the SCN circadian clock network. *Cell* **129:** 605–616.
Lorenz WW, McCann RO, Longiaru M, Cormier MJ. 1991. Isolation and expression of a cDNA encoding Renilla reniformis luciferase. *Proc Natl Acad Sci* **88:** 4438–4442.
Luker KE, Luker GD. 2008. Applications of bioluminescence imaging to antiviral research and therapy: Multiple luciferase enzymes and quantitation. *Antiviral Res* **78:** 179–187.
Manjarrés IM, Chamero P, Domingo B, Molina F, Llopis J, Alonso MT, Garcia-Sancho J. 2008. Red and green aequorins for simultaneous monitoring of Ca^{2+} signals from two different organelles. *Pflugers Arch* **455:** 961–970.
Martin JR, Rogers KL, Chagneau C, Brulet P. 2007. In vivo bioluminescence imaging of Ca^{2+} signalling in the brain of Drosophila. *PLoS ONE* **2:** e275. doi: 10.1371/journal.pone.0000275.
Michelini E, Cevenini L, Mezzanotte L, Ablamsky D, Southworth T, Branchini B, Roda A. 2008. Spectral-resolved gene technology for multiplexed bioluminescence and high-content screening. *Anal Chem* **80:** 260–267.
Mihalcescu I, Hsing W, Leibler S. 2004. Resilient circadian oscillator revealed in individual cyanobacteria. *Nature* **430:** 81–85.
Millar AJ, Short SR, Chua NH, Kay SA. 1992. A novel circadian phenotype based on firefly luciferase expression in transgenic plants. *Plant Cell* **4:** 1075–1087.
Miloud T, Henrich C, Hammerling GJ. 2007. Quantitative comparison of click beetle and firefly luciferases for in vivo bioluminescence imaging. *J Biomed Opt* **12:** 054018.
Nakajima Y, Ikeda M, Kimura T, Honma S, Ohmiya Y, Honma K. 2004a. Bidirectional role of orphan nuclear receptor RORα in clock gene transcriptions demonstrated by a novel reporter assay system. *FEBS Lett* **565:** 122–126.
Nakajima Y, Kimura T, Suzuki C, Ohmiya Y. 2004b. Improved expression of novel red- and green-emitting luciferases of *Phrixothrix* railroad worms in mammalian cells. *Biosci Biotechnol Biochem* **68:** 948–951.
Nakajima Y, Kimura T, Sugata K, Enomoto T, Asakawa A, Kubota H, Ikeda M, Ohmiya Y. 2005. Multicolor luciferase assay system: One-step monitoring of multiple gene expressions with a single substrate. *BioTechniques* **38:** 891–894.
Nakamura M, Maki S, Amano Y, Ohkita Y, Niwa K, Hirano T, Ohmiya Y, Niwa H. 2005. Firefly luciferase exhibits bimodal action depending on the luciferin chirality. *Biochem Biophys Res Commun* **331:** 471–475.
Nguyen VT, Morange M, Bensaude O. 1989. Protein denaturation during heat shock and related stress. *J Biol Chem* **264:** 10487–10492.
Noguchi T, Ikeda M, Ohmiya Y, Nakajima Y. 2008. Simultaneous monitoring of independent gene expression patterns in two types of cocultured fibroblasts with different color-emitting luciferases. *BMC Biotechnol* **8:** 40.
O'Brien MA, Daily WJ, Hesselberth PE, Moravec RA, Scurria MA, Klaubert DH, Bulleit RF, Wood KV. 2005. Homogeneous, bioluminescent protease assays: Caspase-3 as a model. *J Biomol Screen* **10:** 137–148.
Ogura R, Matsuo N, Wako N, Tanaka T, Ono S, Hiratsuka K. 2005. Multicolor luciferases as reporters for monitoring transient gene expression in higher plants. *Plant Biotechnol* **22:** 151–155.
Paguio A, Almond B, Fan F, Stecha P, Garvin D, Wood M, Wood K. 2005. pGL4 vectors: A new generation of luciferase reporter vectors. *Promega Notes* **89:** 7–10.
Plautz JD, Kaneko M, Hall JC, Kay SA. 1997. Independent photoreceptive circadian clocks throughout *Drosophila*. *Science* **278:** 1632–1635.
Rogers KL, Stinnakre J, Agulhon C, Jublot D, Shorte SL, Kremer EJ, Brulet P. 2005. Visualization of local Ca^{2+} dynamics with genetically encoded bioluminescent reporters. *Eur J Neurosci* **21:** 597–610.
Rogers KL, Picaud S, Roncali E, Boisgard R, Colasante C, Stinnakre J, Tavitian B, Brulet P. 2007. Non-invasive in vivo imaging of calcium signaling in mice. *PLoS ONE* **2:** e974. doi: 10.1371/journal.pone.0000974.
Rogers KL, Martin JR, Renaud O, Karplus E, Nicola MA, Nguyen M, Picaud S, Shorte SL, Brulet P. 2008. Electron-multiplying charge-coupled detector-based bioluminescence recording of single-cell Ca^{2+}. *J Biomed Opt* **13:** 031211.
Ruan GX, Allen GC, Yamazaki S, McMahon DG. 2008. An autonomous circadian clock in the inner mouse retina regulated by dopamine and GABA. *PLoS Biol* **6:** e249. doi: 1071.1371/journal.pbio.0060249.

Shaner NC, Campbell RE, Steinbach PA, Giepmans BN, Palmer AE, Tsien RY. 2004. Improved monomeric red, orange and yellow fluorescent proteins derived from Discosoma sp. *Nat Biotechnol* **22:** 1567–1572.

Shimomura O. 2006. *Bioluminescence: Chemical principles and methods.* World Scientific, Hackensack, NJ.

Shimomura O, Musicki B, Kishi Y, Inouye S. 1993. Light-emitting properties of recombinant semi-synthetic aequorins and recombinant fluorescein-conjugated aequorin for measuring cellular calcium. *Cell Calcium* **14:** 373–378.

Shu X, Royant A, Lin MZ, Aguilera TA, Lev-Ram V, Steinbach PA, Tsien RY. 2009. Mammalian expression of infrared fluorescent proteins engineered from a bacterial phytochrome. *Science* **324:** 804–807.

Stables J, Scott S, Brown S, Roelant C, Burns D, Lee MG, Rees S. 1999. Development of a dual glow-signal firefly and *Renilla* luciferase assay reagent for the analysis of G-protein coupled receptor signalling. *J Recept Signal Transduct Res* **19:** 395–410.

Subramanian C, Xu Y, Johnson CH, von Arnim AG. 2004. In vivo detection of protein–protein interaction in plant cells using BRET. *Methods Mol Biol* **284:** 271–286.

Suzuki T, Usuda S, Ichinose H, Inouye S. 2007. Real-time bioluminescence imaging of a protein secretory pathway in living mammalian cells using *Gaussia* luciferase. *FEBS Lett* **581:** 4551–4556.

Tannous BA, Kim DE, Fernandez JL, Weissleder R, Breakefield XO. 2005. Codon-optimized *Gaussia* luciferase cDNA for mammalian gene expression in culture and in vivo. *Mol Ther* **11:** 435–443.

Thompson JF, Hayes LS, Lloyd DB. 1991. Modulation of firefly luciferase stability and impact on studies of gene regulation. *Gene* **103:** 171–177.

Troy T, Jekic-McMullen D, Sambucetti L, Rice B. 2004. Quantitative comparison of the sensitivity of detection of fluorescent and bioluminescent reporters in animal models. *Mol Imaging* **3:** 9–23.

Venisnik KM, Olafsen T, Gambhir SS, Wu AM. 2007. Fusion of *Gaussia* luciferase to an engineered anti-carcinoembryonic antigen (CEA) antibody for in vivo optical imaging. *Mol Imaging Biol* 267–277.

Villalobos V, Naik S, Piwnica-Worms D. 2008. Detection of protein–protein interactions in live cells and animals with split firefly luciferase protein fragment complementation. *Methods Mol Biol* **439:** 339–352.

Viviani VR. 2002. The origin, diversity, and structure function relationships of insect luciferases. *Cell Mol Life Sci* **59:** 1833–1850.

Viviani VR, Bechara EJ, Ohmiya Y. 1999a. Cloning, sequence analysis, and expression of active *Phrixothrix* railroad-worms luciferases: Relationship between bioluminescence spectra and primary structures. *Biochemistry* **38:** 8271–8279.

Viviani VR, Silva AC, Perez GL, Santelli RV, Bechara EJ, Reinach FC. 1999b. Cloning and molecular characterization of the cDNA for the Brazilian larval click-beetle *Pyrearinus termitilluminans* luciferase. *Photochem Photobiol* **70:** 254–260.

Viviani V, Uchida A, Suenaga N, Ryufuku M, Ohmiya Y. 2001. Thr226 is a key residue for bioluminescence spectra determination in beetle luciferases. *Biochem Biophys Res Commun* **280:** 1286–1291.

Welsh DK, Kay SA. 2005. Bioluminescence imaging in living organisms. *Curr Opin Biotechnol* **16:** 73–78.

Welsh DK, Logothetis DE, Meister M, Reppert SM. 1995. Individual neurons dissociated from rat suprachiasmatic nucleus express independently phased circadian firing rhythms. *Neuron* **14:** 697–706.

Welsh DK, Yoo SH, Liu AC, Takahashi JS, Kay SA. 2004. Bioluminescence imaging of individual fibroblasts reveals persistent, independently phased circadian rhythms of clock gene expression. *Curr Biol* **14:** 2289–2295.

Welsh DK, Imaizumi T, Kay SA. 2005. Real-time reporting of circadian-regulated gene expression by luciferase imaging in plants and mammalian cells. *Methods Enzymol* **393:** 269–288.

Wilson T, Hastings JW. 1998. Bioluminescence. *Annu Rev Cell Dev Biol* **14:** 197–230.

Wood KV. 1995. Marker proteins for gene expression. *Curr Opin Biotechnol* **6:** 50–58.

Wood KV, Lam YA, Seliger HH, McElroy WD. 1989. Complementary DNA coding click beetle luciferases can elicit bioluminescence of different colors. *Science* **244:** 700–702.

Yamaguchi S, Isejima H, Matsuo T, Okura R, Yagita K, Kobayashi M, Okamura H. 2003. Synchronization of cellular clocks in the suprachiasmatic nucleus. *Science* **302:** 1408–1412.

Yang KS, Ilagan MX, Piwnica-Worms D, Pike LJ. 2009. Luciferase fragment complementation imaging of conformational changes in the epidermal growth factor receptor. *J Biol Chem* **284:** 7474–7482.

Yoo SH, Yamazaki S, Lowrey PL, Shimomura K, Ko CH, Buhr ED, Siepka SM, Hong HK, Oh WJ, Yoo OJ, et al. 2004. PERIOD2::LUCIFERASE real-time reporting of circadian dynamics reveals persistent circadian oscillations in mouse peripheral tissues. *Proc Natl Acad Sci* **101:** 5339–5346.

Yoo S-H, Yamazaki S, Buhr E, Park J, Kojima S, Green CB, Takahashi JS. 2008. An SV-40 polyadenylation signal sequence in the 3′UTR of Per2::Luciferase(SV) mice lengthens free-running period and increases PER2 (#6). *Soc Res Biol Rhythms Abstr* **20:** 64.

Zhang Y, Phillips GJ, Li Q, Yeung ES. 2008. Imaging localized astrocyte ATP release with firefly luciferase beads attached to the cell surface. *Anal Chem* **80:** 9316–9325.

Zhao H, Doyle TC, Coquoz O, Kalish F, Rice BW, Contag CH. 2005. Emission spectra of bioluminescent reporters and interaction with mammalian tissue determine the sensitivity of detection in vivo. *J Biomed Opt* **10:** 41210.